

Illuminants as visualization tools for clinical diagnostics and surgery

Maritoni Litorja,* Steven W. Brown, Chungsan Lin and Yoshi Ohno
National Institute of Standards and Technology, 100 Bureau Dr., Gaithersburg, MD 20899

ABSTRACT

The requirements for diagnostic and surgical lighting have remained largely unchanged over the past several years—illumination level, glare, shadow and tissue heating reduction are the dominant factors in choosing a lighting system. Since human visual perception remains the key tool in clinical diagnostics and surgery, it is worth exploring ways to heighten visual contrast between areas of interest with respect to surrounding tissues. A simulation program for predicting test illuminant spectral distribution that would enhance contrast between standard color patches typical of tissue color is used. Data images of the color patches under the predicted test illuminant as realized using a spectrally tunable source are collected. Details of the simulation program, the equipment used for this test and results of the test will be discussed.

Keywords: illumination, surgical lighting, color contrast

1. INTRODUCTION

A surgeon's vision is still one of the primary tools in the surgical suite. Most imaging modalities have been developed to extend the human vision to distinguish between normal and non-normal tissues. However, the bulkiness of conventional imaging equipment makes them inappropriate for surgical use. New optical visualization methods, such as those generated from hyperspectral reflectance imaging, can be spectrally manipulated to make certain structures observable. This relies on a camera for acquisition and software for hypercube data manipulation. Here we propose exploring the use of a spectrally shaped illumination source to optimize the contrast between features with subtle color differences commonly encountered in a biomedical setting. It should be noted that this work is instrument and metrics-based, with the awareness that there is a parallel and distinct vision science discipline which explores human visual color perception.^{1,2,3} Since this is a standards and metrics-based approach to exploring color contrast through simulations, the essential tool here is the use of quantitative measures of color according to CIE standards.⁴

There are many examples in the literature on the use of quantitative colorimetry in biomedical applications. It has been used in the study of hyperpigmented spots on the skin and to standardize the measurement of skin color for dermatologic studies.⁵ The main objective is that quantitative color measurement of tissues will lead to standardized tissue imaging, transferability of data for telemedicine and ultimately, a more informed clinical decision. The concept of imaging using selective bands of light is utilized in narrowband imaging,⁶ or alternately known as optimal band imaging.⁷ In selective band imaging, bands of red, green and blue light, at least, are sequentially used to illuminate the biological sample. In the above-mentioned references, they were used to illuminate during endoscopic procedures. The authors show that top layer tissue features and histological patterns show up better under the less penetrating blue light. This information is otherwise washed out using broadband white light illumination due to the higher contribution of red light. This effectively sections the tissues being imaged through differences in penetration depth. This is similar but improves upon chromoendoscopy, which uses dyes to stain the tissue *in vivo* since with selective band imaging, there is no need for dyes, which can prolong a procedure.

* litorja@nist.gov

2. MEASUREMENTS OF ILLUMINATION SOURCES

2.1 Conventional Surgical Light Sources

Overhead surgical lamps are high luminance sources, focusable and adjustable for different zonal lighting purposes, and designed for reduced shadow. White light sources are typically used for diagnostics and surgical lighting. We measured the spectral radiance of a couple of typical overhead surgical lamps^{8†} using a transfer calibration spectroradiometer traceable to the NIST scale for radiance measurements, with a measurement uncertainty not greater than 1% (k=2). Both lamps have five pods each. The first source is a conventional overhead surgical lamp with one quartz halogen bulb in each pod. The second one has four-color light emitting diodes (LEDS) arrayed in a hexagonal pattern in each pod. The second lamp measured is LED-based, with an array of to produce the white light. The LED lamp has four coordinated color temperature (CCT) settings, from 3000 K to 5000 K and five preset power adjustment levels.

The radiance of the each lamp is measured by directing the light onto a standard reference reflectance plaque in normal geometry. Light from all five pods was focused into a single spot, about 10 mm in diameter at the lamp-plaque distance indicated. The spectroradiometer was positioned at a 45° angle from normal.

The results of the spectral radiance measurements for the quartz halogen lamp are presented in Fig. 2.1.1. The lamp-to-plaque distance was 77.5 cm, with the source focused to a single spot. The lamp's rotary dimmer switch was set close to the maximum output of the lamp. Similarly, the results of the spectral radiance measurements of the LED lamp are presented in Fig. 2.1.2 at the highest output levels for color temperature settings 3000 K and 5000 K.

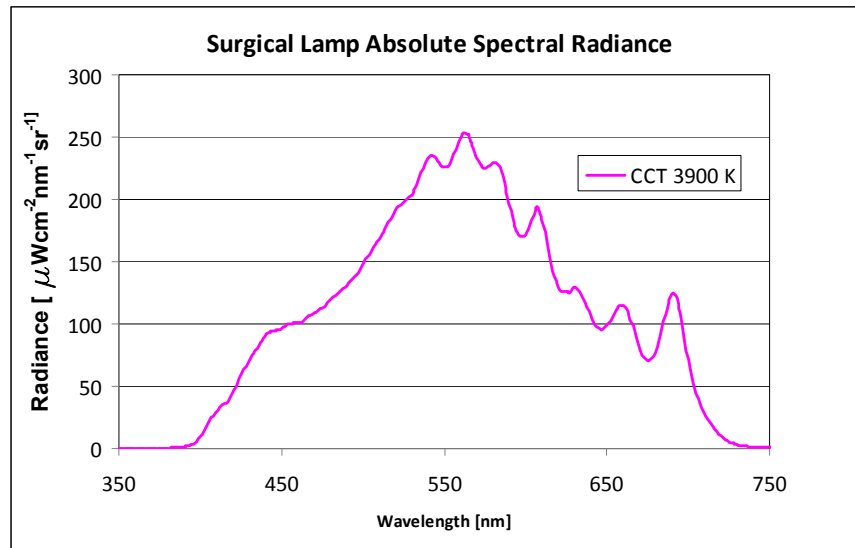


Figure 2.1.1. Results of the spectral radiance measurements of a five-bulb quartz halogen overhead surgical lamp. Lamp-to-plaque distance = 77.5 cm and the lamp output is set at close to maximum of the range.

[†] It should be noted that the identification of commercial equipment is for information purposes only. It does not imply recommendation or endorsement by NIST, nor does it imply that the equipment identified is necessarily the best available for the purpose.

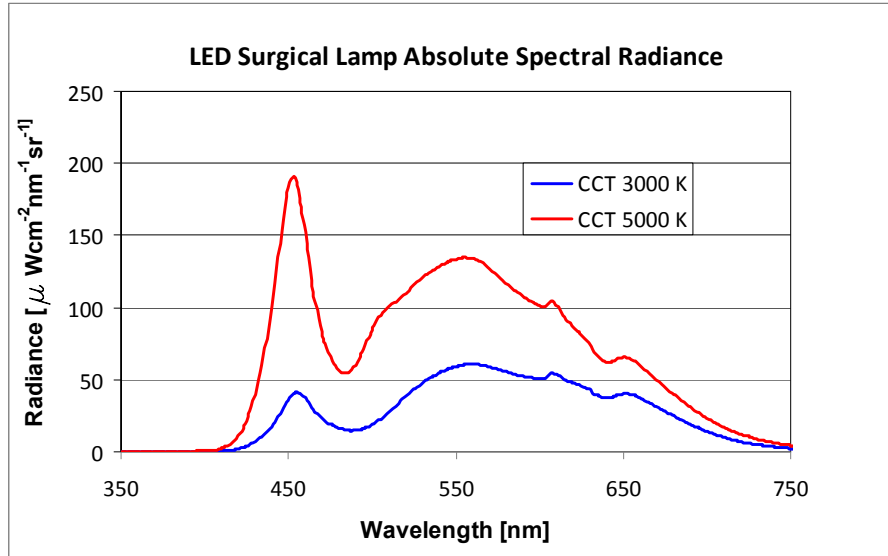


Figure 2.1.2. Spectral radiance measurements of a LED five-pod overhead surgical lamp. The lamp-to-plaque distance was 70.1 mm. The lamp was on the highest output level for both color temperature settings.

2.2 Spectrally Tunable Light Source

A spectrally tunable source consists of a white light source passed through either a prism or grating and the spectrally dispersed light is spatially fitted onto a digital micro-mirror (DMD) array. Each mirror in the array can be selectively turned on or off at a fast rate, thereby allowing selective wavelengths to be produced. The output is delivered via lightguide for various applications. This tunable light source is capable of sweeping through the visible spectral range at greater than 5 kHz. Due to the programmability, any color temperature can be produced and any part of the spectrum can be heightened or suppressed without the need for filters. It is possible to create any spectral distribution for specific applications. This type of source is now commercially available.^{9,10}

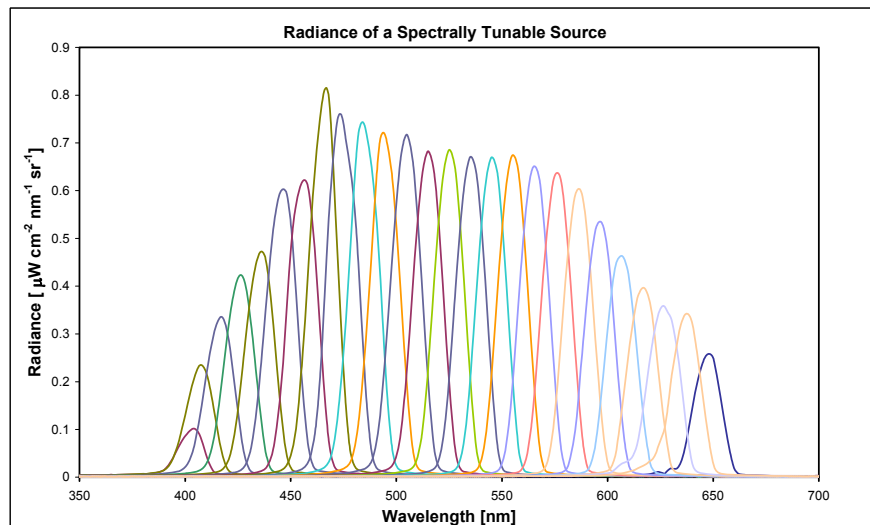


Figure 2.2.1 Spectral radiance measurements of a commercially available spectrally tunable source. All mirrors were turned on, and the overall spectral shape reflects that of the broadband Xe source.

3. COLOR CONTRAST

Metrics for color contrast have been developed over the past few decades, as the practice of photometry was modernized. While colorimetry was a matter of subjective judgment for many industries in the late 1950's, the creation of standards and standards-setting bodies such as the Commission Internationale de l'Eclairage (CIE) has led to uniform color metrics across industries and locales and adoption of technological solutions such as automated colorimeters for many industrial quality assurance procedures.

3.1 NIST Color Quality Simulation Program

The NIST Color Quality Simulation Program software¹¹ was created by Dr. Ohno as an evaluation tool for the various light sources used in industry, especially with the new LED lighting, where spectral ranges for the various component colors may differ according to vendor.

This simulation program (in Excel) provides calculation of color quantities of various lamp spectral distributions including Color Rendering Index (CRI) (CIE 13.3)¹² and the NIST Color Quality Scale (CQS), which is still being refined.¹³ The colors of the 14 Munsell color chips used in CIE 13.3 and the 15 samples used in CQS are presented on the computer screen for both reference and test illuminants. The simulation program uses color conversion from CIE XYZ⁴ to RGB using a chromatic adaptation transform, from different CCT of test sources to D65 (common computer screen illuminant) white point. One of the uses of this simulation program is for optimization modeling of LED light sources. For instance, on the 3-LED model and 4-LED model, just by entering a CCT value, the program automatically does the color mixing of RGB LEDs so that the mixed white light produces the specified CCT exactly on the Planckian locus. This feature allows one to use Excel Solver to optimize LED spectra for maximum luminous efficacy or maximum CRI, etc., under given conditions.

The simulation program has a database of the spectral distributions of many light sources. It also has the stored spectral distributions of reference color samples. It solves for the color of the samples under different test sources, and shows the samples' colors under both reference and test lighting conditions. Reference light sources are normally Daylight, Illuminant A (tungsten lamp) or D65 (computer screen). For this particular application, the spectral distribution of tissue samples, acquired through hyperspectral reflectance imaging, are used in place of the reference color samples. The surgical lighting spectral distributions, described in Section 1.2, as well as other synthesized distributions were added to the simulation program database. In the next section are examples of color patches of sample spectral distribution under various light sources through the simulation. The results from the NIST CQS simulations are for single spatial points only.

3.2 Example of Tissue Color Patches

The tissue examples used here are chosen simply on the basis of hyperspectral image data availability. The simulation program requires spectral reflectance information for the entire visible range of the spectrum in order to predict the colors correctly.

The color differences between sample patches are computed using the CIE L*a*b* (CIELAB) color space.⁴ ΔE^*_{ab} , the magnitude of the color difference between two object colors, and ΔL^* , the magnitude of difference between light and dark, for a pair of samples from a scene are presented in each figure for comparative purposes. Different source spectral distributions were tested to produce various ΔE^*_{ab} , ΔL^* combinations, using the NIST CQS Simulation Program.

Fig. 3.2.1 shows the spectra of a kidney and one of its large blood vessels taken from a previously collected hyperspectral image. The original hyperspectral images were acquired with a CCD camera outfitted with a liquid crystal tunable filter. A Xe lamp was used for illumination and a white reference reflectance plaque for image normalization.¹⁴ The normalized hyperspectral images are then convolved with the desired light source spectral distribution using ENVI software¹⁵ for viewing the whole scene. Color patches of the kidney and blood vessel are presented in Fig. 3.2.2. These are shown pair-wise for viewer comparison since color reproduction is software and equipment-dependent.

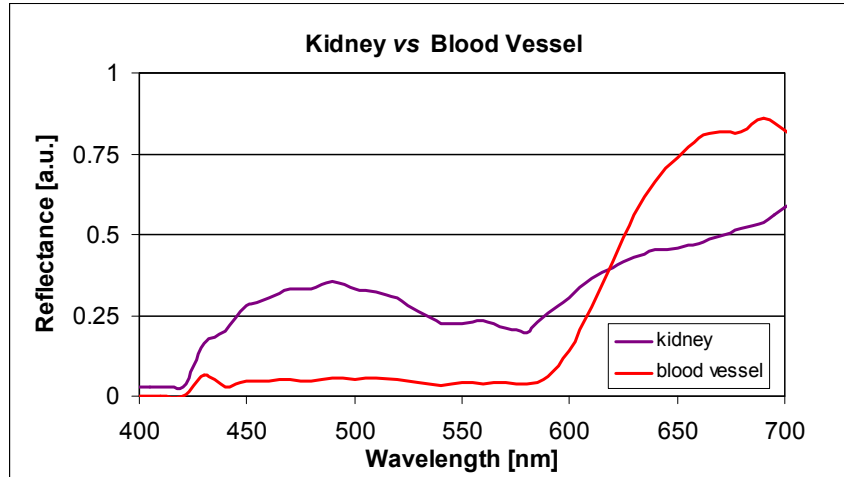


Figure 3.2.1 Reflectance spectra of a kidney and blood vessel perfused with blood

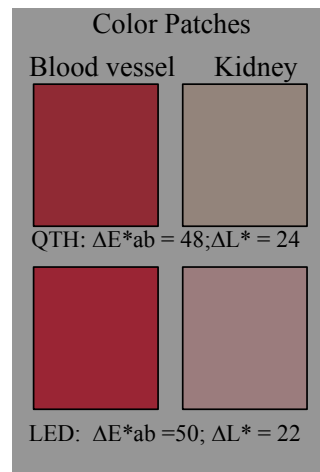


Figure 3.2.2 Color patches of a blood vessel (left) and a kidney (right) perfused with blood under the quartz halogen lamp (top) and the LED surgical lamp (bottom).

In Fig. 3.2.2, the LED lamp (CCT=5000 K), with its higher blue spectral content, affects a higher ΔE^* than the quartz halogen lamp and therefore gives a higher reflectance value to the kidney in contrast to the blood vessel. For tissues such as these, where there is a distinct difference in absorbance/reflectance in one spectral region versus another, it is possible to heighten the reflectance of one tissue type over another by increasing the luminance of the light source to highlight the desired region.

One can select spectral bands and vary the spectral distribution, such as shown in Fig. 3.2.3. A lamp distribution with higher contribution in the blue-green region, with a peak centered at 500 nm, aims to boost the reflectance of the kidney in the blue-green region, and lower the reflectance from the red with a lower luminance contribution from the red region. The colors from such a lamp would have a greenish white-point, and the kidney will appear gray and the blood vessels are red. The color patches are shown in Fig. 3.2.4.

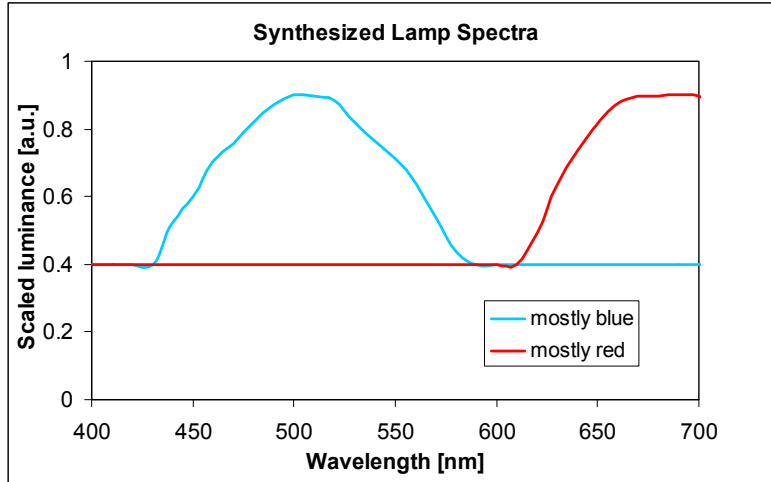


Figure 3.2.3 Synthesized lamp spectral distribution heightening the green region, and suppressing the red region of the spectrum

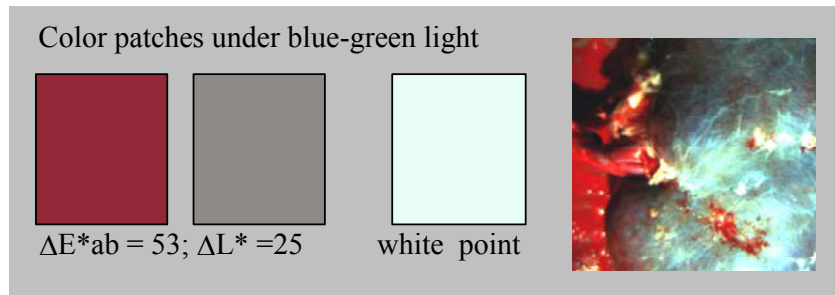


Figure 3.2.4 Colors of the blood vessel and kidney under a simulated lamp spectrum rich in blue. The white appears greenish under this lamp. On the right is the image of the scene under this lamp.

If on the other hand, the red component is heightened and the blue suppressed, using the other spectral distribution in Fig. 3.2.3, results in the color patches shown in Fig. 3.2.5. The whole image generally appears redder. It should be noted that suppressing the red region entirely would not give any advantage in contrast since both tissues have high reflectance in the red region. It will only result in the whole scene appearing dim. Comparing the two spectral compositions, while the mostly red light results in a larger ΔE^* than the blue-green light, the ΔL^* value is lower than that with the blue-green light. This is simply to illustrate that these are the types effects that are possible when illumination can be spectrally tuned. The luminance levels of the blue-green and red can be refined to increase both ΔE^* and ΔL^* .

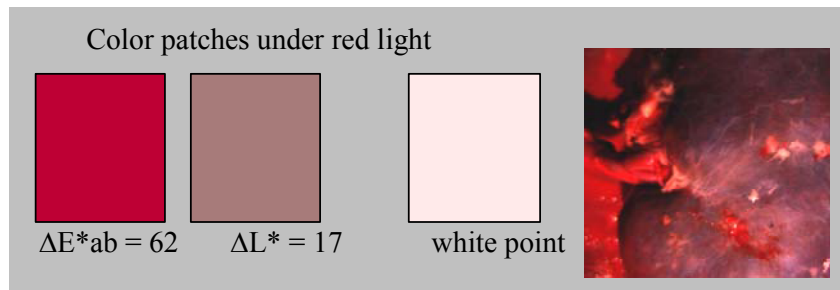


Figure 3.2.5 Colors of the blood vessel and kidney under a lamp distribution richer in red

The next figure two points on the dorsal side of a forearm; one from a region over a vein, and one from an adjacent patch of normal skin. Fig. 3.2.6 show the reflectance spectra of these two regions. They differ simply from the reflectance values primarily due to differences in the magnitude of absorbance of light in the visible region by hemoglobin. Fig. 3.2.7 shows the color patches of these two areas under the quartz halogen and LED lamps.

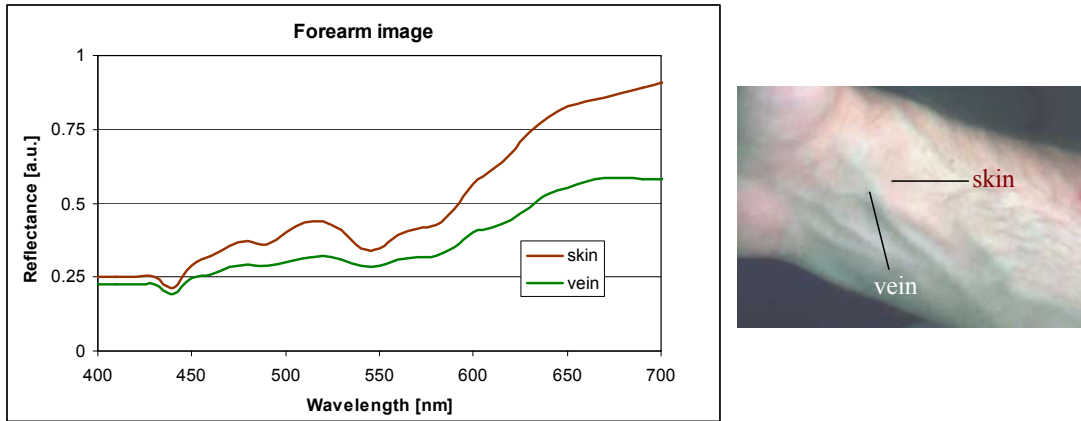


Figure 3.2.6 Reflectance spectra of skin on the dorsal side of a forearm and the image under the LED lamp.

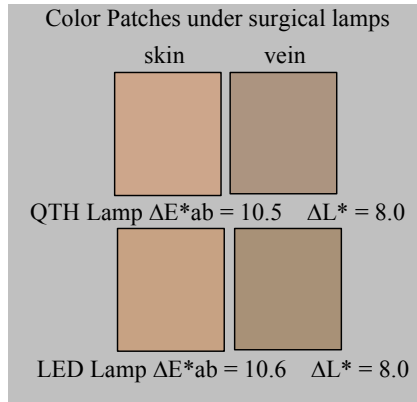


Figure 3.2.7 Colors of normal skin (left) and that of a patch over a vein (right), under the quartz halogen lamp (top) and the LED surgical lamp (bottom) at color temperature of 5000 K.

Using the synthetic lamp distributions in Fig. 3.2.3, one peaked in the blue-green centered at 500 nm and another at 680 nm results in the colors in Fig. 3.2.8.

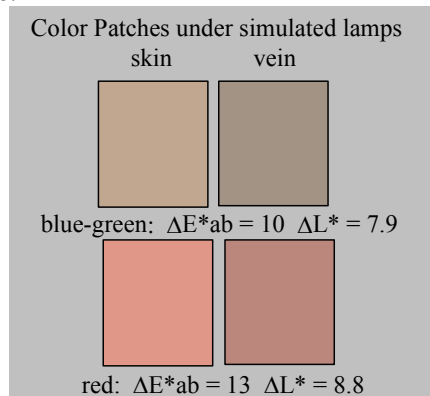


Figure 3.2.8 Color patches when using the spectral distributions of mostly blue-green (top) and mostly red (bottom) light source in Fig. 3.2.3.

A section of the spectrum can be suppressed by turning off mirrors of the spectrally tunable light mimicking that of having a color filter. For instance, for the spectrum above for skin and vein, the section around 550 nm can be suppressed entirely, to maximize the difference between the two patches.

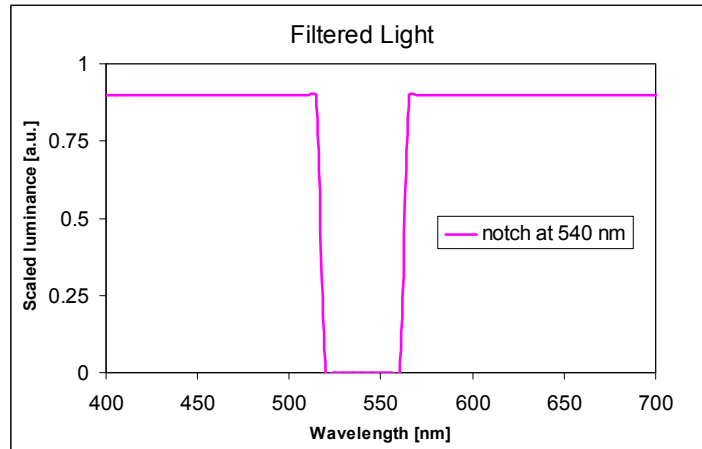


Figure 3.2.9 Light from a selected band can be suppressed by turning off mirrors of the spectrally tunable source

The image in Fig. 3.2.10 are photographs taken with a digital camera of the back of a hand illuminated with a white light and that of the white light with a 50-nm band centered at 540 nm suppressed. The mirrors of the spectrally tunable light engine corresponding to the 515-565 nm region were turned off. The vein structures appear darker compared to the surrounding area.



Figure 3.2.10 Digital photographs of the back of a hand illuminated by white light (left) and white light with a band in the green region suppressed.

4. DISCUSSION

The examples shown above, while not exhibiting dramatic enhancements in contrast, are used to illustrate that it is possible to adjust visual contrast through changes in the light spectral distribution. It is feasible to build such task-specific lighting since the technology for spectrally tunable light is currently available and there are existing metrics that can be used for optimization. The challenge is to find the best metric suitable for tissue colors.

Two sets of data are needed to explore this area further: 1) hyperspectral reflectance data of representative tissue samples from diagnostic and surgical scenes and 2) contrast metrics specific to tissue colors. Certain difficulties arise in the acquisition of hyperspectral reflectance data. Unlike data acquired for analyte determinations, where only signals at certain specific wavelengths are needed, data cubes for color analysis have to be collected over the full visible spectrum range, from 400 nm to 700 nm, at a fixed source-observer geometry, to avail of standard metrics published by the CIE. Surgical lamps are still mostly of the quartz halogen type, with little contribution in the blue region. CCD cameras typically have poor responsivity in the blue. If the data collection is done improperly, the poor signals in the blue region

result in incorrect color upon analysis. A visual perception study involving clinical practitioners would be very beneficial and will provide the second set of information needed.

The reflectance factors of tissues are slow-varying over the visible range and the bandwidths of chromophores that lend color are large. So, only specific spectral regions may need to be enhanced, depending on the types of tissues, and this can be met by using color LEDs to boost certain spectral bands. Some current commercial surgical lamps use blue LEDs to enhance the color temperature. However, color temperature is not necessarily the important aspect of the illuminant that will enhance the clinician's vision. It is possible to provide a clinician another adjustment to enhance his/her vision beyond just luminance level.

Color and luminance are just a couple of the tools mentioned here for extending visualization of normal vs. non-normal tissues using optical methods. Recent advances in hyperspectral imaging, such as quantitative measurements of oxygenation in tissues and use of fluorescent tags on anomalous tissues can be coupled with the concept of selective spectral lighting such as that shown in this paper to enhance the contrast between the features of interest amid surrounding tissues.

Acknowledgements: The authors thank Dr. Wendy Davis at NIST for technical advice on color contrast techniques.

REFERENCES

-
- [1.] Hashimoto, K. and Nayatani, Y. "Visual Clarity and Feeling of Contrast", *Color Research and Applications*, 19(3), 171, (1994).
 - [2.] Lotto, R.B. and Purves, D. "An empirical explanation of color contrast", *Proc. Nat. Acad. Sci.* 97(23), 12834, (2000).
 - [3.] Abrams, A., Hillis, J. and Brainard, D. "The relation between color discrimination and color constancy: when is optimal adaptation task dependent?" *Neural Computation*, 19, 2610, (2007).
 - [4.] Commission Internationale de l'Eclairage. *Colorimetry, CIE 15: (2004)*.
 - [5.] Miyamoto, K., Takiwaki, H., Hillenbrand, G.G., Arase, S. "Development of a digital imaging system for objective measurement of hyperpigmented spots on the face", *Skin Res. Technol.*, 8(4) 227, 2002; *Bioengineering of the Skin: Skin Imaging and Analysis*, 2ed. Wilhelm, K.P. *et al*, editors, 209, CRC Press, (2006).
 - [6.] Hamamoto, Y., Endo, T., Noshio, K., Arimura, Y., Sato, M. and Imai, K. "Usefulness of Narrowband imaging endoscopy for diagnosis of Barrett's esophagus", *J. Gastroenterol.*, 39, 14, (2004).
 - [7.] Cammarota, G. Cesaro, P. Cazzato, A. Fedeli, P. Sparano, L. Vecchio, F.M. Larroca, L.M. and Gasbarrini, G. "Optimal band imaging system: a new tool for enhancing the duodenal villous pattern in celiac disease", *Gastrointest. Endosc.* 68(2), 352, (2008).
 - [8.] Courtesy of the laboratory of Dr. Alex Gorbach, National Institutes of Health, Bethesda, MD.
 - [9.] One Light Corporation's One Light Spectra. <http://www.onelightcorp.com/index.html>
 - [10.] Optronics Laboratories' OL490. <http://www.olinet.com/>
 - [11.] Ohno, Y. and Davis, W., NIST CQS Simulation 7.4, NIST Optical Technology Division, Gaithersburg, MD.
 - [12.] Commission Internationale de l'Eclairage. *Method of Measuring and Specifying Colour Rendering Properties of Light Sources, CIE 13.3, (1995)*.
 - [13.] Davis, W. and Ohno, Y., "Toward an improved color rendering metric", in *Fifth International Conference on Solid State Lighting*, Ed. Ferguson, I. T. Carrano, J. C., Taguchi, T, Ashdown, I.E., *Proc. SPIE 5941, 59411G*, (2005).
 - [14.] Litorja, M., Brown, S.W., Nadal, M. and Allen, D.W. "Development of Surgical Lighting for Enhanced Color Contrast", *Proc. SPIE 6515, 65150K*, (2007).
 - [15.] ENVI 4.4 Software. ITT Industries Inc., <http://www.itvis.com/envi/index.asp>